Description of superdeformed nuclear states in the interacting boson model

Yu-xin Liu,[1,2,3,4] Jian-gang Song,[2] Hong-zhou Sun,[5,3] and En-guang Zhao[1,3]
[1]*CCAST (World Laboratory), P. O. Box 8730, Beijing 100080, China*
[2]*Department of Physics, Peking University, Beijing 100871, China*
[3]*Institute of Theoretical Physics, Academia Sinica, P. O. Box 2735, Beijing 100080, China*
[4]*Institut für Theoretische Physik, Universität Tübingen, Auf der Morgenstelle 14, D-72076 Tübingen, Germany*
[5]*Department of Physics, Tsinghua University, Beijing 100084, China*
(Received 31 March 1997)

We show in this paper that the superdeformed nuclear states can be described with a four parameter formula in the spirit of the perturbated SU(3) limit of the sdg IBM. The $E2$ transition γ-ray energies, the dynamical moments of inertia of the lowest superdeformed (SD) bands in even-even Hg, Pb, Gd, and Dy isotopes, and the energy differences $\Delta E_\gamma - \Delta E_\gamma^{\rm ref}$ of the SD band 1 of ^{194}Hg are calculated. The calculated results agree with experimental data well. This indicates that the SD states are governed by a rotational interaction plus a perturbation with $\mathrm{SO}_{sdg}(5)$ symmetry. The perturbation causing the $\Delta I=4$ bifurcation to emerge in the $\Delta I=2$ superdeformed rotational band may then possess $\mathrm{SO}_{sdg}(5)$ symmetry. [S0556-2813(97)01509-4]

PACS number(s): 21.10.Re, 21.60.Fw, 23.20.Lv, 27.80.+w

I. INTRODUCTION

Since the discovery of the first discrete superdeformed (SD) rotational band in the nucleus ^{152}Dy [1] in 1986, the investigation of superdeformation at high angular momenta remains one of the most interesting and challenging topics of nuclear structure. The detailed experimental investigation of superdeformation (for a review on the data see the compilation in Ref. [2]) reveals many interesting properties of the SD bands such as the phenomenon of the identical band [3], $\Delta I=4$ bifurcation (many experimental results and theoretical investigations are available now: for experiments see, for example, Refs. [4–10]; for theory see, for example, Refs. [11–18]), and the turnover of the dynamical moment of inertia $\mathcal{J}^{(2)}$ with rotational frequency $\hbar\omega$ [5]. By now, it is commonly accepted that the properties of the SD bands, such as the dependence of $\mathcal{J}^{(2)}$ on $\hbar\omega$, depend sensitively on the number of occupied high-N intruder orbitals. On the microscopic side, the density-dependent Hartree-Fock calculation with zero range forces of the Skyrme type [19] or with finite range forces of the Goney type [20] and calculations with the cranked relativistic mean field theory [21] have been performed. In these models, the bulks and the single-particle properties are treated consistently based on the concept of variation principle, however, the price to be paid is a higher numerical effort. With this in mind there are so far not many applications available yet. Based on the semiphenomenological approach (the cranked Nilsson-Strutinsky and cranked Woods-Saxon-Strutinsky approach) [22], many calculations (for instance, Refs. [23,24]) have been accomplished (for a review, see Refs. [22] and [25]) and many experimental manuscripts also contain applications of these models to the latest experimental data. By treating the bulks and single-particle properties separately they have the advantage of fitting many details of the actual nuclei under investigation directly to the appropriate region under study. Since the rich variety of physical phenomena in the region of superdeformed shapes is based on a complicated and rather subtle interplay of collective and single-particle properties, the numerical calculation within the framework is also quite time consuming. Moreover, the agreement between the calculated results and the experimental data still has room for improvement.

On the phenomenological side, many models [26–29] have also been proposed with different microscopic or semimicroscopic foundations. Because of the rich underlying physics and the conciseness of calculation, the interacting boson model (IBM) [30] has also been extended to describe SD states [31,32]. In the SD IBM, all the group structure and techniques are the same as those in the usual IBM. However, from the Nilsson model we know that states with large deformation and high spins can be described only by the inclusion of many spherical shells, the number of bosons is then much larger for superdeformed states than for normally deformed states (2–4 times or more) [31,32]. More recent investigations [32–35] indicated that g bosons (the $L=4$ nucleon pairs) in the IBM play a much more significant role in describing SD states than in describing normally deformed states. Especially, Ref. [32] indicated that the SU(3) limit of the sdg IBM is a reasonable starting point to describe SD states in the IBM. Reference [33] showed that there exists a basis and a Hamiltonian within the sdg IBM which reproduces the geometric model results [11–13] for the $\Delta I=4$ bifurcation (in other words, the $\Delta I=2$ staggering of E_γ energies or dynamical moments of inertia) [4–10] and Ref. [34] pointed out that the perturbated SU(3) limit may be a suitable candidate to describe the valuable insight of the dynamics of SD states. Otherwise the spin dependence of the $\mathcal{J}^{(2)}$ of SD states is treated by introducing a spin-dependent strength (referred to as the Arima coefficient) for the interaction with SO(3) symmetry $(\hat{L}\cdot\hat{L})$ [36]. However, numerical calculation shows that the $\mathcal{J}^{(2)}$ obtained from the IBM with an Arima coefficient changes monotonously with rotational frequency. Then the turnover can not be described. In this paper, by employing the perturbated $\mathrm{SU}_{sdg}(3)$ symmetry in the sdg IBM and extending the Arima coefficient, we discuss the properties of the SD states of the even-even nu-

clei in the $A\sim190$ and $A\sim150$ regions. In particular, the turnover of the dynamical moment of inertia with rotational frequency and the $\Delta I=4$ bifurcation will be investigated.

The paper is organized as follows. In Sec. II a short description of the possibility that SD states can be described on a firmer foundation within the perturbated $\mathrm{SU}_{sdg}(3)$ symmetry with perturbation holding the $\mathrm{SO}_{sdg}(5)$ symmetry is presented and a four parameter formula is developed by extending the Arima coefficient and considering the perturbation. In Sec. III numerical results for the lowest SD bands of the even-even nuclei in the $A\sim190$ and 150 regions are described and discussed. Finally conclusion and remarks are given in Sec. IV.

II. FORMALISM

In the sdg interacting boson model [37,38], the collective nuclear states (with quadrupole and hexadecupole deformations) are generated as states of a system with N s, d, and g bosons. Since the total single boson space is 15 dimensional, the symmetry group is U(15). It has strong coupling dynamical symmetries SU(3), SU(5), SU(6), O(15) and weak coupling dynamical symmetries $\mathrm{U}_{sd}(6)\otimes\mathrm{U}_{g}(9)$, $\mathrm{U}_{dg}(14)$, $\mathrm{U}_{d}(5)\otimes\mathrm{U}_{sg}(10)$. It has been shown [32,34] that the $\mathrm{SU}_{sdg}(3)$ limit could provide a reasonable phenomenological framework for superdeformed nuclear states.

As a nucleus holds the SU(3) symmetry of the sdg IBM, the states of the nucleus can be classified by the irreducible representations (irreps) of the group chain

$$U_{sdg}(15)\supset \mathrm{SU}_{sdg}(3)\supset \mathrm{SO}_{sdg}(3). \tag{1}$$

The wave functions are

$$\begin{array}{lllll} |\psi(I)\rangle=|[N]_{15} & \alpha & (\lambda,\mu) & K & I\rangle \\ \quad \mathrm{U}_{sdg}(15), & & \mathrm{SU}(3), & & \mathrm{SO}_{sdg}(3), \end{array} \tag{2}$$

where α and K are the additional quantum numbers. All the irreps and additional quantum numbers can be determined with the branching rules [38] of the irrep reductions. And the interaction Hamiltonian of the nucleus can be written as

$$H=\epsilon C_{1\mathrm{U}_{sdg}(15)}+\kappa C_{2\mathrm{SU}_{sdg}(3)}+CC_{2\mathrm{SO}_{sdg}(3)}, \tag{3}$$

in which C_{kG} is the k-order Casimir operator of the group G. The energy of the state $|[N]_{15}\alpha(\lambda,\mu)KI\rangle$ is

$$E(I)=E_0+\epsilon N+\kappa[\lambda^2+\mu^2+\lambda\mu+3(\lambda+\mu)]+CI(I+1). \tag{4a}$$

Considering only the relative excitation of the states in a rotational band, the energy of the state with angular momentum I can be simply expressed as

$$E(I)=CI(I+1). \tag{4b}$$

With the spin dependence of the dynamical moment of inertia being considered, Eq. (3) should be rewritten as

$$H=\epsilon C_{1\mathrm{U}_{sdg}(15)}+\kappa C_{2\mathrm{SU}_{sdg}(3)}+\frac{C_0}{1+fC_{2\mathrm{SO}_{sdg}(3)}}C_{2\mathrm{SO}_{sdg}(3)}, \tag{5}$$

in which the parameter f can be regarded as the Arima coefficient. The energy of the state I in a band is given as

$$E(I)=\frac{C_0}{1+fI(I+1)}I(I+1). \tag{6}$$

Numerical calculation shows that the $\mathcal{J}^{(2)}$ obtained in this way changes with $\hbar\omega$ monotonously. Then, the recently observed turnover [2,5,10] of the $\mathcal{J}^{(2)}$ with $\hbar\omega$ in experiment cannot be described with Eqs. (5) and (6).

Along the line of the variable moment of inertia (VMI) model [39], we expand the Arima coefficient f as $f=f_1+f_2C_{2\mathrm{SO}_{sdg}(3)}$. Equation (5) can then be rewritten as

$$H=\epsilon C_{1\mathrm{U}_{sdg}(15)}+\kappa C_{2\mathrm{SU}_{sdg}(3)}+\frac{C_0}{1+f_1C_{2\mathrm{SO}_{sdg}(3)}+f_2(C_{2\mathrm{SO}_{sdg}(3)})^2}C_{2\mathrm{SO}_{sdg}(3)}. \tag{7}$$

The energy of the state I in a band is given as

$$E(I)=\frac{C_0}{1+f_1I(I+1)+f_2I^2(I+1)^2}I(I+1). \tag{8}$$

As the parameters f_1 and f_2 are taken as $f_1>0$, $f_2<0$ (or $f_1<0$, $f_2>0$), Eqs. (7) and (8) generate the rotational band which exhibits turnover or platform of the $\mathcal{J}^{(2)}$ with $\hbar\omega$ pretty well. However, the obtained dynamical moment of inertia changes with rotational frequency so smooth that the quite weak $\Delta I=2$ staggering (for example, in Refs. [5,10]) cannot be reproduced. Then, to describe the turnover and the $\Delta I=2$ staggering of dynamical moment of inertia with rotational frequency simultaneously, the SU(3) symmetry must be broken down. On the other hand, experimental data indicate that superdeformed nuclear states are mainly governed by rotational characteristic plus some components of other deformations. It indicates that the breaking down of the SU(3) symmetry is quite slight, so that only an appropriate perturbation should be added to Eq. (7).

On the other hand, many investigations on the other aspects of the sdg IBM have been accomplished. In view of the geometric shape, by employing the coherent state technique [30], Devi and Kota [40] showed that the geometric shape of the $\mathrm{SU}_{sdg}(5)$ limit of the sdg IBM is relevant for deformed nuclei as well as the $\mathrm{SU}_{sdg}(3)$ limit. However, its stable shape is not oriented at $\gamma=0°$ but at $\gamma=60°$. In the view of other variables, calculations on the hexadecupole deformation parameter β_4 [41], the two nucleon transfer cross section [42], and energy spectra [40,35] indicated that the $\mathrm{SU}_{sdg}(5)$ limit has almost the same property in describing deformed rotational nuclear states as the $\mathrm{SU}_{sdg}(3)$ does. Moreover, the potential energy surface of the nucleus with the $\mathrm{SU}_{sdg}(5)$ symmetry via its intrinsic deformation variable β_4 has two minima that are displayed in energy [40]. This indicates that the $\mathrm{SU}_{sdg}(5)$ symmetry of the sdg IBM admits shape coexistence and shape phase transformation which can be driven by hexadecupole deformation or angular momentum. Combining these facts with the well-known idea that superdeformed nuclear states are the ones generated in the second minimum of the potential energy surface, we know

TABLE I. Parameters used in the calculation (B and C_0 in keV).

	$f_2 \neq 0$				$f_2 = 0$		
	B	C_0	f_1	f_2	B	C_0	f_1
^{190}Hg	0.001136	6.027	8.314×10^{-5}	-8.562×10^{-9}	-0.002062	5.963	6.378×10^{-5}
^{192}Hg	0.001887	5.706	7.827×10^{-5}	-9.108×10^{-9}	0.001326	5.605	4.585×10^{-5}
^{194}Hg	0.0005095	5.618	7.097×10^{-5}	-6.842×10^{-9}	0.002550	5.515	4.284×10^{-5}
^{192}Pb	0.006755	5.860	1.151×10^{-4}	-2.813×10^{-8}	0.003875	5.758	7.335×10^{-5}
^{194}Pb	0.001681	5.688	8.182×10^{-5}	-1.375×10^{-8}	0.002313	5.601	5.275×10^{-5}
^{196}Pb	-0.0005568	5.709	5.137×10^{-5}	-1.808×10^{-9}	-0.0008264	5.699	4.756×10^{-5}
^{198}Pb	0.005425	5.725	4.336×10^{-5}	-4.229×10^{-9}	0.002556	5.695	3.074×10^{-5}
^{148}Gd	0.002965	5.248	-2.862×10^{-5}	1.427×10^{-9}	0.0002014	5.354	-1.836×10^{-5}
^{150}Gd	-0.001187	5.634	2.181×10^{-5}	-2.894×10^{-9}	0.0007603	5.255	-4.510×10^{-6}
^{152}Dy	-0.0001534	5.393	-1.042×10^{-5}	5.817×10^{-10}	0.0002124	5.443	-6.127×10^{-6}
^{154}Dy	-0.001103	5.480	-9.184×10^{-6}	5.845×10^{-10}	0.0001570	5.536	-4.785×10^{-6}

TABLE II. Calculated γ-ray energies of the SD bands of Hg isotopes and the comparison with experiment.

	^{190}Hg		^{192}Hg		^{194}Hg(1)		
Spin	Exp. [a]	Cal.	Exp. [b]	Cal.	Exp. [a]	Exp. [c]	Cal.
10			214.4(3)	213.8			
12			257.8(1)	257.2	254.3(1)	253.93(4)	253.72
14	316.9(4)	316.1	300.1(1)	299.7	296.4(1)	295.99(3)	295.85
16	360.0(2)	359.7	341.4(1)	341.4	337.6(1)	337.18(3)	337.12
18	402.34(04)	402.1	381.6(1)	381.8	377.7(1)	377.39(3)	377.40
20	442.98(06)	443.3	421.1(2)	421.3	416.9(1)	416.60(3)	416.68
22	482.71(06)	483.2	458.8(2)	459.6	454.9(1)	454.76(3)	454.86
24	521.30(06)	521.8	496.0(2)	496.9	492.1(1)	491.86(5)	492.00
26	558.6(1)	559.0	532.1(2)	532.9	528.0(1)	527.88(3)	528.00
28	594.9(1)	595.0	567.4(2)	568.0	563.0(1)	562.92(3)	562.98
30	630.1(1)	630.0	601.7(2)	601.9	596.9(1)	596.87(5)	596.88
32	664.1(1)	663.9	634.9(2)	635.2	630.1(1)	629.93(3)	629.87
34	696.9(1)	696.6	668.1(2)	667.5	662.2(1)	662.07(4)	661.92
36	728.5(4)	728.6	700.1(2)	699.4	693.6(1)	693.40(4)	693.24
38	757.4(4)	759.8	731.5(2)	730.6	724.2(1)	723.91(6)	723.82
40	783.5(6)	790.6	762.3(3)	761.8	754.2(1)	753.92(6)	753.95
42			792.7(4)	792.7	783.9(1)	783.67(8)	783.63
44			822.9(4)	824.0	813.5(2)	813.12(3)	813.18
46			853.1(5)	855.6	842.8(3)	842.55(6)	842.65
48			888.7(7)	888.3	872.6(5)	872.41(13)	872.39
50					903.5(8)	903.10(18)	902.47

[a]References [2,5].
[b]Reference [43].
[c]Reference [10].

TABLE III. Calculated γ-ray energies of the SD bands of Pb isotopes and the comparison with experiment.

	^{192}Pb		^{194}Pb		^{196}Pb		^{198}Pb	
Spin	Exp. [a]	Cal.	Exp. [a]	Cal.	Exp. [a]	Cal.	Exp. [b]	Cal.
6			124.9(5)	124.5				
8			169.6(2)	169.1	171.0(2)	170.3		
10			213.4(1)	213.1	215.1(3)	214.9		
12	262.6(4)	262.0	256.4(1)	256.3	258.9(2)	259.1		
14	304.1(4)	304.4	298.6(1)	298.6	302.4(3)	302.6	305.1	304.5
16	345.6(4)	345.8	339.8(1)	340.0	345.3(3)	345.4	348.3	348.1
18	385.6(3)	385.7	380.2(1)	380.4	387.3(3)	387.5	391.1	390.8
20	424.4(4)	424.7	419.3(2)	419.8	428.3(3)	428.7	432.6	433.2
22	462.8(5)	462.3	458.2(1)	458.1	468.8(3)	469.0	473.9	474.5
24	500.0(6)	499.4	495.4(1)	495.6	508.2(4)	508.2	515.0	515.5
26	535.1(8)	535.3	532.1(2)	532.0	546.4(4)	546.5	555.2	555.3
28	570.6(11)	571.4	568.4(2)	567.7	584.2(4)	583.6	594.9	594.9
30	604	606.8	602.7(1)	602.7	620.0(4)	619.7	633.6	633.3
32	636	643.2	638.1(4)	637.4	654.6(4)	654.6	671.9	671.5
34			672.3(4)	671.7	688.6(4)	688.4	709.9	708.5
36			706.2(2)	706.1	720.1(7)	721.0	747.3	745.7
38			739.5(4)	740.6	752.1(8)	752.5	781.7	781.6
40							818.8	817.8
42							850.5	853.0

[a]Reference [2].
[b]Reference [44].

TABLE IV. Calculated γ-ray energies of the SD bands of Gd and Dy isotopes and the comparison with experiment (the experimental data are taken from Ref. [2]).

	^{148}Gd		^{150}Gd		^{152}Dy		^{154}Dy	
Spin	Exp.	Cal.	Exp.	Cal.	Exp.	Cal.	Exp.	Cal.
28					602.4(1)	602.1		
30					647.5(1)	647.2		
32	699.8(4)	697.7			692.7(1)	692.6		
34	747.3(4)	746.6			738.1(1)	738.2	749.0(3)	748.0
36	796.7(4)	796.7	780.0(10)	768.1	784.0(1)	784.1	794.4(2)	794.2
38	846.6(4)	847.2	815.0(4)	809.1	829.9(1)	830.3	840.6(2)	840.7
40	897.9(4)	899.0	848.9(1)	849.9	876.481)	876.7	887.4(2)	887.3
42	950.1(4)	951.3	888.0(1)	890.9	923.2(1)	923.4	933.5(2)	934.2
44	1003.9(6)	1004.8	928.9(1)	931.9	970.2(1)	970.3	981.1(1)	981.2
46	1058.4(6)	1058.9	970.9(4)	973.3	1017.4(1)	1017.5	1028.2(2)	1028.5
48	1114.3(6)	1114.2	1013.4(2)	1014.9	1064.9(1)	1064.9	1075.8(2)	1075.8
50	1170.6(6)	1169.8	1056.2(1)	1057.3	1112.7(1)	1112.6	1123.8(2)	1123.5
52	1227.6(6)	1226.8	1099.7(1)	1100.1	1160.5(1)	1160.4	1171.1(2)	1171.0
54	1285.2(6)	1284.0	1144.1(3)	1144.0	1208.6(1)	1208.4	1218.7(2)	1218.9
56	1343.7(6)	1342.4	1190.4(1)	1188.7	1256.6(1)	1256.5	1266.7(2)	1266.6
58	1402.9(5)	1400.9	1237.6(1)	1234.9	1304.8(1)	1304.7	1315.1(2)	1314.6
60	1461.7(5)	1460.5	1286.3(2)	1282.3	1352.9(1)	1353.0	1361.9(3)	1362.3
62	1520.0(6)	1519.9	1336.8(2)	1331.8	1401.3(1)	1401.4	1410.2(5)	1410.1
64	1579.6(9)	1580.3	1387.0(2)	1382.9	1449.6(2)	1449.7	1457.5(6)	1457.6
66			1439.3(3)	1436.7	1497.8(3)	1497.9	1503.7(7)	1505.2
68			1492.4(3)	1492.9	1545.6(5)	1546.0		

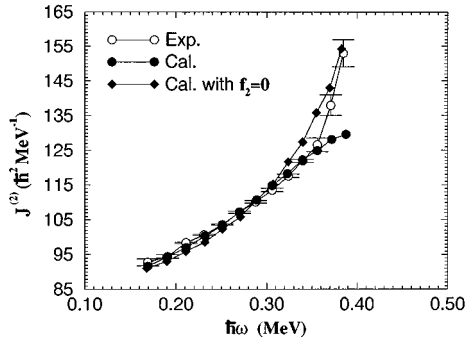

FIG. 1. The calculated result of the dynamical moments of inertia as a function of the rotational frequency of the SD band 1 of ^{190}Hg and the comparison with experiment. The experimental data are taken from Ref. [2].

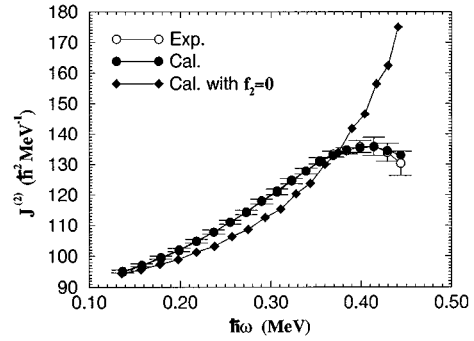

FIG. 3. The same as Fig. 1 but for the SD band 1 of ^{194}Hg. The experimental data are taken from Ref. [10].

that the $\mathrm{SU}_{sdg}(5)$ symmetry of the sdg IBM may be also a good candidate to describe superdeformed rotational states. Furthermore the spectrum generating process shows that the irrep $[n_1,n_2,n_3,n_4]$ of $\mathrm{SU}_{sdg}(5)$ plays the same role in labeling the states as the irrep (λ,μ) of $\mathrm{SU}_{sdg}(3)$ does, and it does not contribute to the excitation energy of the state in a band labeled by it. The most significant difference between the $\mathrm{SU}_{sdg}(5)$ limit and the $\mathrm{SU}_{sdg}(3)$ limit is then the term of interaction with $\mathrm{SO}_{sdg}(5)$ symmetry. Therefore it is quite sophisticated if an interaction with $\mathrm{SO}_{sdg}(5)$ symmetry is added as a perturbation to the Hamiltonian (7). We get then

$$H=\epsilon C_{1\mathrm{U}_{sdg}(15)}+\kappa C_{2\mathrm{SU}_{sdg}(5)}+BC_{2\mathrm{SO}_{sdg}(5)}+\frac{C_0}{1+f_1C_{2\mathrm{SO}_{sdg}(3)}+f_2(C_{2\mathrm{SO}_{sdg}(3)})^2}C_{2\mathrm{SO}_{sdg}(3)}. \quad (9)$$

The excited energy of the state with angular momentum I in a SD band is thus given as

$$E(I)=B[\tau_1(\tau_1+3)+\tau_2(\tau_2+1)]+\frac{C_0}{1+f_1I(I+1)+f_2I^2(I+1)^2}I(I+1). \quad (10)$$

Comparing Eq. (9) with Eq. (7), we know that the $\mathrm{SU}_{sdg}(3)$ is changed to $\mathrm{SU}_{sdg}(5)$ besides a term $BC_{2\mathrm{SO}_{sdg}(5)}$ being added. It seems at first glance that the interaction Hamiltonian has been changed completely, however, they are, in fact, almost equivalent to each other in describing SD rotational band in the view of the above discussion except for the perturbation. It is certain that, to guarantee that the interaction with $\mathrm{SO}_{sdg}(5)$ symmetry is only a perturbation, we should preserve very small $|B|\ll C_0,|f_1|$, and $|f_2|$.

Summarizing the previous discussions we know that by perturbating the $\mathrm{SU}_{sdg}(3)$ symmetry of the sdg IBM and extending the Arima coefficient, the excitation energy of the state in a SD band is given with a four parameter formula [Eq. (10)]. With the four parameter formula, the $E2$ transition γ-ray energy $E_\gamma(I)=E(I)-E(I-2)$, the rotational frequency $\hbar\omega(I)=[E_\gamma(I)+E_\gamma(I+2)]/4$ and the dynamical moment of inertia $\mathcal{J}^{(2)}=4\hbar^2/[E_\gamma(I+2)-E_\gamma(I)]$ can consequently be determined. Moreover, the energy differences ΔE_γ between two consecutive γ-ray transitions after subtraction of a smooth reference $\Delta E_\gamma^{\mathrm{ref}}(I)$ can also be obtained. Taking Cederwall's notation, we have

$$\Delta E_\gamma(I)-\Delta E_\gamma^{\mathrm{ref}}(I)=\frac{3}{8}\left\{E_\gamma(I)-\frac{1}{6}[4E_\gamma(I-2)+4E_\gamma(I+2)-E_\gamma(I-4)-E_\gamma(I+4)]\right\}. \quad (11)$$

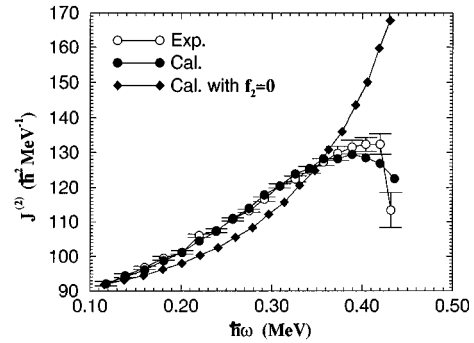

FIG. 2. The same as Fig. 1 but for ^{192}Hg. The experimental data are taken from Ref. [43].

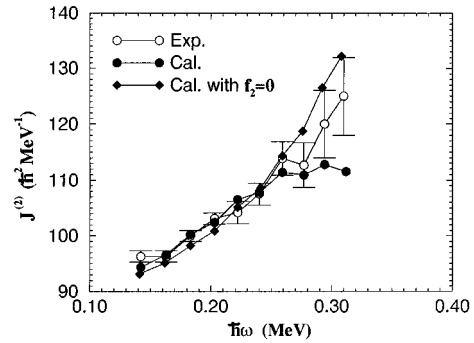

FIG. 4. The same as Fig. 1 but for ^{192}Pb. The experimental data are taken from Ref. [2].

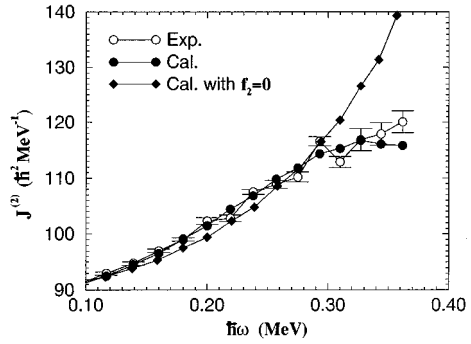

FIG. 5. The same as Fig. 1 but for ^{194}Pb. The experimental data are taken from Ref. [2].

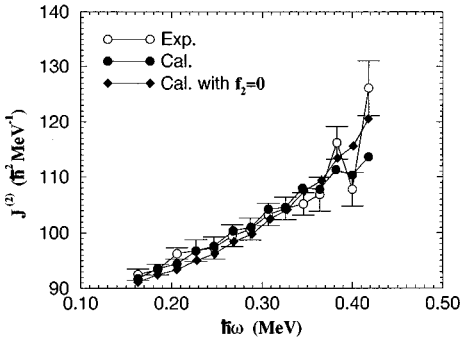

FIG. 7. The same as Fig. 1 but for ^{198}Pb. The experimental data are taken from Ref. [44].

It is also necessary to mention that to demonstrate the $\Delta I=4$ bifurcation in experiment, one expresses the ΔE_γ as a function of the rotational frequency [4–10] since the angular momenta are not assigned. However, in a theoretical description, it can be illustrated as a function of the rotational frequency or the angular momentum [11–18]. Qualitative calculation [35] shows that, only if the parameters hold relation $|B|\ll C$ [the case of $f_1=f_2=0$ in Eq. (10)], the variation characteristic of $\Delta E_\gamma(I)-\Delta E_\gamma^{\mathrm{ref}}(I)$ as a function of angular momentum is consistent with that as a function of rotational frequency. We now turn our discussion to the changing feature of the $\Delta E_\gamma(I)-\Delta E_\gamma^{\mathrm{ref}}(I)$ versus the rotational frequency $\hbar\omega$ in the practical calculation of this paper.

III. CALCULATION AND DISCUSSION

Investigating the above formalism more carefully, we know that the four parameter formula [Eq. (10)] can only be used for positive parity states in even-even nuclei. However, experiment shows that there are also many SD bands with negative parity. To describe the negative parity states in IBM, f bosons should be taken into account. Then the group chain which classifies the wave functions of the states must be rewritten. Considering the lower excitation which includes only one f boson, the group chain and the corresponding irreps can be given as

U(22)$\supset$	U$_{sdg}$(15)	$\otimes$U$_f$(7)	$\supset$SU$_{sdg}$(3)	$\otimes$SU$_f$(7)	$\supset$SO$_{sdg}$(3)	$\otimes$SO$_f$(7)	$\supset$SO$_{sdg}$(3)	$\otimes$SO$_f$(3)	$\supset$SO(3),
$[N]$	$[N_{sdg}]_{15}$	$[1]_7$	(λ,μ)	$[1]_7$	I_{sdg}	$(1)_7$	I_{sdg}	3	I

with perturbation

U(22)	$\supset$U$_{sdg}$(15)	$\otimes$U$_f$(7)	$\supset$SU$_{sdg}$(5)	$\otimes$SU$_f$(7)	$\supset$SO$_{sdg}$(5)	$\otimes$SO$_f$(7)	$\supset$SO$_{sdg}$(3)	$\otimes$SO$_f$(3)	$\supset$SO(3),
$[N]$	$[N_{sdg}]_{15}$	$[1]_7$	$[n_1,n_2,n_3,n_4]_5$	$[1]_7$	$(\tau_1,\tau_2)_5$	$(1)_7$	I_{sdg}	3	I.

It shows that for a state with definite angular momentum I, the angular momentum contributed by the s, d, and g bosons can be $I_{sdg}=I-3,I-2,I-1,I,I+1,I+2,I+3$ and the number of the s, d, and g bosons is $N_{sdg}=N-1$, where N is the

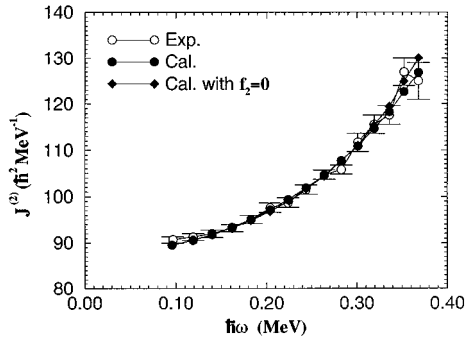

FIG. 6. The same as Fig. 1 but for ^{196}Pb. The experimental data are taken from Ref. [2].

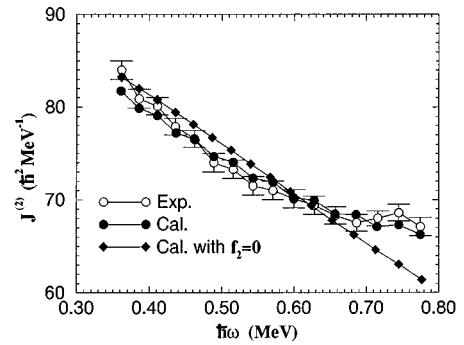

FIG. 8. The same as Fig. 1 but for ^{148}Gd. The experimental data are taken from Ref. [2].

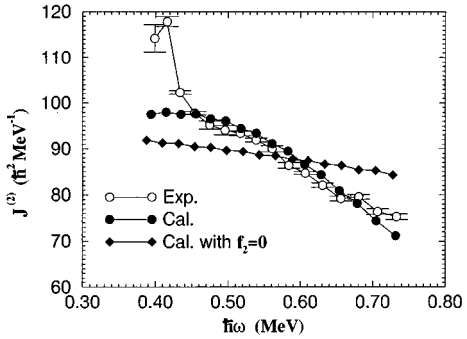

FIG. 9. The same as Fig. 1 but for ^{150}Gd. The experimental data are taken from Ref. [2].

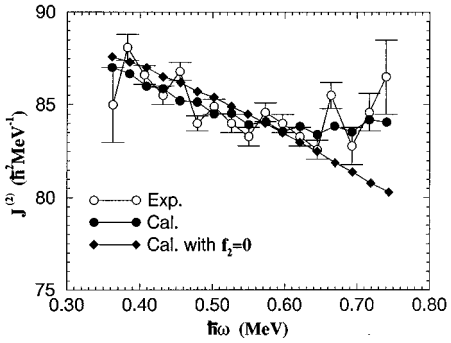

FIG. 11. The same as Fig. 1 but for ^{154}Dy. The experimental data are taken from Ref. [2].

total boson number determined by the shell structure. Then we can take $I=I_{sdg}$ for simplicity but pay no attention to the exact boson number and the parity when we regard Eq. (10) as a four parameter formula to fit experimental data. In fact, in view of the last section, the boson number does not contribute directly to the excitation energy of the state in a SD band except for the influence on the angular momentum. In practical calculations, the angular momentum is assigned with the guidance of experimental data. The irrep (τ_1,τ_2) of the $SO_{sdg}(5)$ in Eq. (10) is determined by the branching rules of the irrep reduction [38]. What we used in calculation can be simply given as

$$(\tau_1,\tau_2) = \begin{cases} \left(\frac{I}{2},0\right), & \text{if } I=4k,4k+1 (k+0,1,2,\ldots), \\ \left(\frac{I}{2}-1,2\right), & \text{if } I=4k+2,4k+3 (k=0,1,2,\ldots). \end{cases}$$

After a nonlinear least fitting to the experimentally observed E_γ energies, we get the spin assignment and the $E2$ transition γ-ray energies. The best fitted parameters are listed in Table I. It shows that the practical value of the B is only $C_0/1000$ or even less, i.e., the interaction with the $SO_{sdg}(5)$ symmetry is really only a perturbation. The calculated results of the E_γ energies and the comparison with experimental data are listed in Tables II, III, and IV for the SD bands in Hg, Pb, Gd, and Dy isotopes, respectively. With

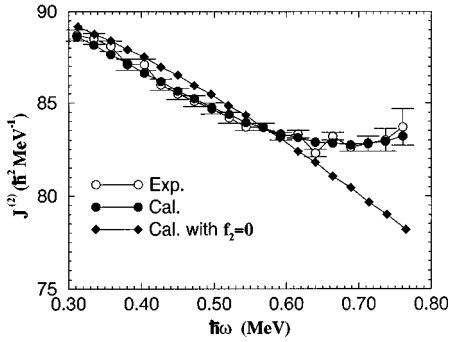

FIG. 10. The same as Fig. 1 but for ^{152}Dy. The experimental data are taken from Ref. [2].

$\mathcal{J}^{(2)}=4\hbar^2/[E_\gamma(I+2)-E_\gamma(I)]$, the dynamical moments of inertia of the above SD bands are also obtained. The calculated results and comparison with experimental data are illustrated in Figs. 1–11. For comparison, we give also the calculated results in the case with $f_2=0$ and where the $E2$ γ-ray energies are reproduced well.

From the figures we know that the smooth increase of the dynamical moment of inertia with rotational frequency in the Hg-Pb region is reproduced well in both the $f_2\neq 0$ and $f_2=0$ cases. In more detail, the case of $f_2=0$ is favored for the monotonous increase at higher rotational frequency in the SD bands of ^{190}Hg and ^{192}Pb, but fails to reproduce the changing feature of the SD bands of ^{192}Hg, ^{194}Hg, and ^{194}Pb, which exhibit a turnover or platform in the changing curve of the $\mathcal{J}^{(2)}$ vs $\hbar\omega$. For the SD bands in the Gd-Dy region, the experimentally observed dynamical moment of inertia changes much more smoothly with rotational frequency than that in the Hg-Pb region, and holds a platform or even a turnover. Figures 8–11 show that only if $f_2\neq 0$, can the changing characteristic be depicted well. In particular, if $f_2=0$, the obtained dynamical moment of inertia $\mathcal{J}^{(2)}$ of ^{150}Gd is almost a constant. Only if $f_2\neq 0$, can the experimentally observed feature of the $\mathcal{J}^{(2)}$ of ^{150}Gd be reproduced. However, the SD bands of ^{144}Gd and ^{146}Gd cannot be described well not only with $f_2=0$ but also with $f_2\neq 0$ because there are sudden jumps in $\mathcal{J}^{(2)}$ which are probably due to sudden particle alignment [45].

For the $\Delta I=4$ bifurcation, since there is not a definite conclusion for band 2 and band 3 of ^{194}Hg and the phase

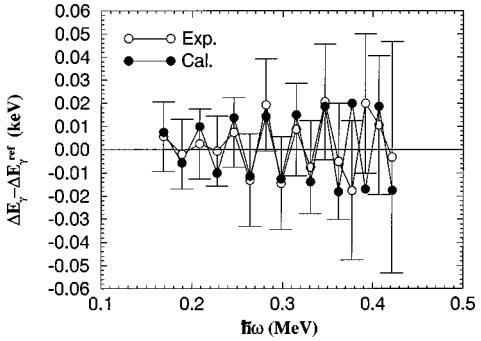

FIG. 12. The calculated result of the energy differences ΔE_γ as a function of rotational frequency of the SD band 1 of ^{194}Hg and the comparison with experiment. The experimental data are taken from Ref. [10].

shifts are quite complicated in these two bands [10], we show then only the calculated result of $\Delta E_\gamma - \Delta E_\gamma^{\rm ref}$ against the rotational frequency of the SD band 1 in ^{194}Hg in Fig. 12. It indicates that the experimentally observed staggering is well reproduced in our approach except for the phase shift at about $\hbar\omega = 0.38$–0.39 MeV.

Investigating the tables and the Figs. 1–11, we know that the $E2$ transition γ-ray energies and the dynamical moment of inertia of the SD states can be quantitatively described excellently when the f_2 is not taken as zero. In particular, the turnover or the platform can be reproduced well. However, as the parameter $f_2 = 0$, the turnover cannot be depicted. To discuss the mechanism for why the turnover of $\mathcal{J}^{(2)}$ with $\hbar\omega$ is described well in our approach, we compare it with a rigid rotor. It is known that the energy of a rigid rotor is given as $E_{\rm rot} = (\hbar^2/2\mathcal{J})I(I+1)$. Its dynamical moment of inertia is a constant $\mathcal{J}$. When the energy of the state is given as Eq. (10) with $|B| \ll C_0$, $|f_1|$, and $|f_2|$ very small, the dynamical moment of inertia of the state I is

$$\mathcal{J}^{(2)} \approx \frac{\hbar^2[1+6f_1 I(I+1)+15f_2 I^2(I+1)^2]}{2C_0} \approx \frac{\hbar^2}{2C_0}\left\{1+\frac{3f_1\hbar^2\omega^2}{2C_0^2}[1+4f_1 I(I+1)]+\frac{15f_2\hbar^4\omega^4}{16C_0^4} \times[1+8f_1 I(I+1)]\right\}.$$

It is obvious that when $f_2 = 0$, the angular momentum has a driving (restraining) effect on the $\mathcal{J}^{(2)}$ if $f_1 > 0$ ($f_1 < 0$), and the $\mathcal{J}^{(2)}$ changes monotonously with $\hbar\omega$. If the parameters are taken as $f_1 > 0$, $f_2 > 0$ (or $f_1 < 0$, $f_2 < 0$), the angular momentum driving effect (or the restraining effect) is strengthened. Then $\mathcal{J}^{(2)}$ changes more rapidly with $\hbar\omega$. As they are taken as $f_1 > 0$, $f_2 < 0$ (or $f_1 < 0$, $f_2 > 0$), both the driving effect and the restraining effect are considered, and the competition between them determines the changing characteristic. If the driving effect is stronger, $\mathcal{J}^{(2)}$ increases with $\hbar\omega$. If the restraining effect is stronger, the $\mathcal{J}^{(2)}$ decreases while $\hbar\omega$ increases. When these two effects are in balance with each other, an extreme value appears. Then a turnover emerges. In the present case, the parameters are taken as $f_1 > 0$, $f_2 < 0$ for Hg and Pb isotopes and $f_1 < 0$, $f_2 > 0$ for ^{148}Gd, ^{152}Dy, and ^{154}Dy, respectively, and $|f_1| \gg |f_2|$. Since $|f_2|[I(I+1)]^2$ increases more rapidly than $|f_1|I(I+1)$ as I increases, the two kinds of effects change from driving dominant to restraining dominant in the SD states of Hg-Pb isotopes and from restraining dominant to driving dominant for ^{148}Gd and $^{152-154}$Dy, respectively, a turnover point must then emerge. It is also worthwhile to mention that the best fitted parameters for ^{150}Gd are $f_1 > 0$, $f_2 < 0$, which are the same as those for the Hg and Pb isotopes. This suggests then that the property of ^{150}Gd may be similar to that in the range beyond the turnover of Hg-Pb isotopes, but not close to its neighbors. Comparing the results of $f_2 \neq 0$ with those obtained with $f_2 = 0$, we know that the competition between the driving effect and the restraining effect plays a crucial role in reproducing the turnover. It shows also that the larger one of $|f_1|I(I+1)$ and $|f_2|I^2(I+1)^2$ in Eq. (10) determines the slope of the $\mathcal{J}^{(2)}$ curve with $\hbar\omega$ and the smaller one (f_1 and f_2 take opposite symbols to each other) has an opposite effect and reproduces the turnover.

In a microscopic point of view, Ref. [36] has shown that, as the interaction is written as Eq. (5) with $f > 0$, the term $fI(I+1)$ in the denominator plays a role of antipairing. Extending this idea we know that, as $f < 0$, the term $fI(I+1)$ has a pairing favorite effect. Then, when the Hamiltonian is taken as Eqs. (7), (9) and the parameters are taken as $f_1 > 0$, $f_2 > 0$ (or $f_1 < 0$, $f_2 < 0$), the antipairing (or pairing favorite) effect is strengthened. As they are taken as $f_1 > 0$, $f_2 < 0$ (or $f_1 < 0$, $f_2 > 0$), both the antipairing and pairing effects are taken into account, and the competition between them determines the changing characteristic. The successful description of the dynamical moment of inertia within this approach suggests that there exists competition, even a change over between pairing and quasiparticle alignment caused by the Coliolis antipairing interaction in the SD states in both the $A \sim 190$ and $A \sim 150$ regions.

Recalling the spectrum generating process we know that the totally symmetric irreps $(\tau_1, 0)$ of the $\mathrm{SO}_{sdg}(5)$ generate rotational bands with level sequences $\{0,4,8,12,\ldots\}$, $\{2,6,10,\ldots\}$, etc, and the nontotally symmetric irreps $(\tau_1, 2)$ of the $\mathrm{SO}_{sdg}(5)$ produce bands with level sequences $\{6,10,14,18,\ldots\}$, $\{8,12,16,20,\ldots\}$, etc. According to the rules of sdg IBM, there are strong $E4$ transitions between the states $I+4$ and I which belong to the same kind of SO(5) irreps $(\tau_1+2, 2)$, $(\tau_1, 2)$ [or $(\tau_1+2, 0)$, $(\tau_1, 0)$] separately. Strong $E2$ transition can take place between the states $I+2$ and I which belong to a different kind of SO(5) irreps $(\tau_1, 2)$, $(\tau_1, 0)$ [or $(\tau_1+2, 0)$, $(\tau_1, 2)$]. Thus, two closely placed energy bands with level sequences I_0, I_0+4, I_0+8, . . . , and I_0+2, I_0+6, I_0+10, . . . , appear naturally, and couple to one band with level sequence I_0, I_0+2, I_0+4, ... In this band the states differing by 2 in angular momentum are linked with strong $E2$ transitions. From Eq. (10) we know that the contribution of the term $CI(I+1)$ to $E_\gamma = E(I) - E(I-2)$ is smooth, and that the contribution of the term with SO(5) symmetry is $E_\gamma^{\mathrm{SO}(5)}(I=4k) = (2I-4)B$ and $E_\gamma^{\mathrm{SO}(5)}(I=4k+2) = 6B$. Therefore, there exists E_γ staggering in the SD band, even though the exact value of $|B|$ is very small. This indicates that the simultaneous appearance of the totally and nontotally symmetric irreps in the sdg IBM, which is not possible in the sd IBM, generates the spectrum with $\Delta I = 4$ bifurcation. In other words, it shows that the emergence of the energy band with $\Delta I = 4$ bifurcation is an intrinsic property of the perturbation with the $\mathrm{SO}_{sdg}(5)$ symmetry. From Fig. 12 we know that the feature of the staggering of $\Delta E_\gamma(I) - \Delta E_\gamma^{\rm ref}(I)$ obtained in this spirit agrees with experimental data quantitatively well.

Since the parameter $C = C_0/1 + f_1 C_{2\mathrm{O}(3)} + f_2[C_{2\mathrm{O}(3)}]^2$ in Eq. (9) holds the SO(3) symmetry and the parameters used in practical calculations keeping the relation $|B| \ll C$, the interaction Hamiltonian we used is definitely an axial rotational interaction plus a perturbation with SO(5) symmetry. The successful description of $E_\gamma(I)$, $\mathcal{J}^{(2)}(I)$, and $\Delta E_\gamma(I) - \Delta E_\gamma^{\rm ref}(I)$ implies that the interaction generating the superdeformed rotational bands is governed by the rotational in-

teraction, and the perturbation causing the $\Delta I=2$ rotational band to split into $\Delta I=4$ bifurcation may possess $SO_{sdg}(5)$ symmetry.

IV. CONCLUSION AND REMARKS

In summary, we have shown in this paper that the superdeformed nuclear states can be described in the framework of an interacting boson model as the g bosons are taken into account. By perturbating the $SU_{sdg}(3)$ symmetry with an interaction holding the $SO_{sdg}(5)$ symmetry and extending the Arima coefficient to two coefficients f_1 and f_2, the energies of the states in a SD rotational band are expressed as a four parameter formula with two terms. The first term $B[\tau_1(\tau_1+3)+\tau_2(\tau_2+1)]$ holds the $SO_{sdg}(5)$ symmetry, and determines the $\Delta I=2$ staggering. The second term $C_0/[1+f_1I(I+1)+f_2I^2(I+1)^2]I(I+1)$ possesses SO(3) symmetry and a many-body interaction, and dominates the general characteristic of the band and the changing feature of the dynamical moment of inertia with rotational frequency. With the Arima coefficient being extended to two coefficients f_1 and f_2, both the angular momentum driving and restraining effects on the dynamical moment of inertia and the competition between them can be taken into account simultaneously. On the other hand, along the same line suggested in Ref. [36] we know that the $f_1I(I+1)$ and $f_2I^2(I+1)^2$ in the denominator play roles of antipairing ($f_1>0,f_2>0$) or pairing ($f_1<0,f_2<0$) favored effects and the competition between the paring and antipairing effects is taken into account when f_1 and f_2 are taken with different symbols. However, a more sophisticated microscopic foundation of the parameters remains to be clarified.

With the four parameter formula, we have calculated the $E2$ transition γ-ray spectra and the dynamical moments of inertia of the lowest SD bands in Hg, Pb, Gd, and Dy isotopes and the energy differences $\Delta E_\gamma-\Delta E_\gamma^{\mathrm{ref}}$ of the SD band 1 of ^{194}Hg. The calculated results agree with experimental data excellently, especially the turnover or the platform of the $\mathcal{J}^{(2)}$ with $\hbar\omega$ is reproduced well. It indicates thus that a superdeformed rotational band with $\Delta I=4$ bifurcation can be described well in the sdg IBM as the Hamiltonian is taken as a rotational interaction plus a perturbation with $SO_{sdg}(5)$ symmetry. This provides also a clue that the perturbative interaction making the $\Delta I=2$ superdeformed rotational band split into $\Delta I=4$ bifurcation may possess $SO_{sdg}(5)$ symmetry. The electromagnetic transition rates and the moments of deformations can be given in principle; work to do so is currently in progress. Meanwhile, the applications to other SD bands are also underway. Furthermore, the investigation of describing the SD states in the framework of perturbated SU(3) symmetry with SU(3) wave functions [34] is also being carried out.

ACKNOWLEDGMENTS

This work is supported by the National Natural Science Foundation of China. This work has benefited from stimulating discussions with Professor F. Iachello. Helpful discussions with Professor Qi-zhi Han and Professor C. S. Wu are acknowledged with thanks. The authors are also indebted to Professor A. Faessler for his careful reading of the manuscript. One of the authors (Y.L.) also thanks the support of the Krupp Stiftung and the hospitality of the Institut für Theoretische Physik der Universität Tübingen.

[1] P. J. Twin *et al.*, Phys. Rev. Lett. **57**, 811 (1986).
[2] Xiaoling Han and Chengli Wu, At. Data Nucl. Data Tables **63**, 117 (1996).
[3] R. V. F. Jansseens and T. L. Khoo, Annu. Rev. Nucl. Part. Sci. **41**, 439 (1991).
[4] S. Flibotte *et al.*, Phys. Rev. Lett. **71**, 4299 (1993).
[5] B. Cederwall *et al.*, Phys. Rev. Lett. **72**, 3150 (1994).
[6] B. Cederwall *et al.*, Phys. Lett. B **346**, 244 (1995).
[7] G. Angelis *et al.*, Phys. Rev. C **53**, 679 (1996).
[8] S. M. Fischer *et al.*, Phys. Rev. C **53**, 2126 (1996).
[9] S. M. Semple *et al.*, Phys. Rev. Lett. **76**, 3671 (1996).
[10] R. Krücken *et al.*, Phys. Rev. C **54**, R2109 (1996).
[11] I. Hamamoto and B. R. Mottelson, Phys. Lett. B **333**, 294 (1994); Phys. Scr. **T56**, 27 (1995).
[12] A. O. Macchiavelli *et al.*, Phys. Rev. C **51**, R1 (1995).
[13] I. M. Pavlichenkov and S. Flibotte, Phys. Rev. C **51**, R460 (1995).
[14] F. Dönau, S. Frauendrof, and J. Meng, Phys. Lett. B **387**, 667 (1996).
[15] Y. Sun, J. Y. Zhang, and M. Guidry, Phys. Rev. Lett. **75**, 3398 (1995); Phys. Rev. C **54**, 2967 (1996).
[16] W. D. Luo, A. Bougueffoucha, J. Dobaczewiski, J. Dudek, and X. Li, Phys. Rev. C **52**, 2989 (1995).
[17] P. Magierski, P.-H. Heenen, and W. Nazarewicz, Phys. Rev. C **51**, 2880 (1995); P. Magierski, K. Burzyński, E. Perlińska, J. Dobaczewiski, and W. Nazarewicz, *ibid.* **55**, 1236 (1997).
[18] I. M. Pavlichenkov, Phys. Rev. C **55**, 1275 (1997).
[19] See, for example, P. Bonche, S. J. Krieger, P. Quentin, M. S. Weise, J. Meyer, M. Meyer, N. Redon, H. Flocard, and P. H. Heenen, Nucl. Phys. **A500**, 308 (1989); J. Dobazewski and J. Dudek, Phys. Rev. C **52**, 1827 (1995).
[20] See, for example, M. Girod, J. P. Delaroche, D. Goney, and J. F. Berger, Phys. Rev. Lett. **62**, 2452 (1989); J. L. Egido, L. M. Robledo, and R. R. Chasman, Phys. Lett. B **322**, 22 (1994).
[21] A. V. Afanasjev, J. König, and P. Ring, Nucl. Phys. **A608**, 107 (1996).
[22] S. Åberg, H. Flocard, and W. Nazarewicz, Annu. Rev. Nucl. Part. Sci. **40**, 439 (1990).
[23] M. A. Riley *et al.*, Nucl. Phys. **A512**, 178 (1990).
[24] W. Satula and R. Wyss, Phys. Rev. C **50**, 2888 (1994).
[25] I. Ragnarssen, Nucl. Phys. **A557**, 167c (1993).
[26] C. S. Wu, J. Y. Zeng, Z. Xing, X. Q. Chen, and J. Meng, Phys. Rev. C **45**, 261 (1992).
[27] Jimin Hu and Furong Xu, Phys. Rev. C **48**, 2270 (1993); **49**, 1449 (1994); **52**, 431 (1995).
[28] N. V. Zamfir and R. F. Casten, Phys. Rev. Lett. **75**, 1280 (1995).
[29] L. A. Wu, H. M. Ding, Z. T. Yan, and G. Liu, Phys. Rev. Lett. **76**, 4132 (1996).

[30] F. Iachello and A Arima, *The Interacting Boson Model* (Cambridge University Press, Cambridge, 1987).
[31] F. Iachello, Nucl. Phys. **A522**, 83c (1991); A. Gelberg, P. von Brentano, and R. F. Casten, J. Phys. G **16**, L143 (1990); T. Otsuka and M. Honma, Phys. Lett. B **268**, 305 (1991); H. C. Chiang *et al.* (private communication).
[32] S. Kuyucak, M. Honma, and T. Otsuka, Phys. Rev. C **53**, 2194 (1996).
[33] V. K. B. Kota, Phys. Rev. C **53**, 2550 (1996).
[34] F. Iachello (private communication).
[35] Y. X. Liu, H. Z. Sun, and E. G. Zhao, Commun. Theor. Phys. **27**, 71 (1997).
[36] N. Yoshida, H. Sagawa, T. Otsuka, and A. Arima, Phys. Lett. B **256**, 129 (1991).
[37] A. Bohr and B. R. Mottelson, Phys. Scr. **22**, 468 (1980); **25**, 28 (1982).
[38] H. Z. Sun, M. Moshinsky, A. Frank, and P. van Isacker, Kinam **5**, 135 (1983); V. K. B. Kota, H. De Meyer, J. Vander Jeugt, and G. Vanden Berghe, J. Math. Phys. (N.Y.) **28**, 1644 (1987).
[39] M. A. J. Mariscotti, G. Scharff-Goldhaber, and B. Ruck, Phys. Rev. **178**, 1864 (1969); D. Bonotsos and A. Klein, Phys. Rev. C **29**, 1879 (1984).
[40] Y. D. Devi and V. K. B. Kota, Z. Phys. A **337**, 15 (1990).
[41] Y. D. Devi and V. K. B. Kota, Phys. Rev. C **46**, 370 (1992).
[42] Y. D. Devi and V. K. B. Kota, J. Phys. G **17**, L185 (1991).
[43] P. Fallon *et al.*, Phys. Rev. C **51**, R1609 (1995).
[44] I. M. Hibbert *et al.*, Phys. Rev. C **54**, 2263 (1996).
[45] S. Lunardi *et al.*, Phys. Rev. Lett. **72**, 1427 (1994).